

A New 3D Organization of Mesopores in Oriented CTAB Silica Films

Sophie Besson,^{†,‡} Christian Ricolleau,[§] Thierry Gacoin,[†] Catherine Jacquiod,[‡] and Jean-Pierre Boilot^{*,†}

Groupe de Chimie du Solide, Laboratoire de Physique de la Matière Condensée, UMR CNRS 7643, Ecole Polytechnique, 91128 Palaiseau, France, Laboratoire CNRS/Saint-Gobain "Surface du Verre et Interfaces", UMR CNRS 125, 39 quai Lucien Lefranc, 93303 Aubervilliers, France, and Laboratoire de Minéralogie Cristallographie de Paris, UMR CNRS 7590, Universités Paris VI et Paris VII, 4 place Jussieu, 75252 Paris Cedex 05, France

Received: July 25, 2000

Highly organized and textured CTAB templated silica films are made by the spin-coating technique. The HRTEM structural characterization of these films clearly shows the formation of a 3D hexagonal structure ($P6_3/mmc$ space group) due to the stabilization of a new phase which does not belong to the phase diagram of CTAB in water. This probably results from the formation in dynamic conditions of a 3D-hexagonal packing of spherical micelles separated by polymeric silica walls. The shrinkage of spin-coated films during the drying leads to values of the c/a hexagonal ratio weaker than the one corresponding to the close packed hexagonal structure. This 3D organization is maintained after removal of the surfactant molecules by calcination, leading to a new mesoporous material.

Since their discovery in 1992,¹ structured mesoporous materials synthesized via the polymerization of inorganic species around an organic template have been the subject of much research. They form a new class of very interesting materials, as they have a large surface area and a narrow pore size distribution, which can be adjusted from 2 to 10 nm when using cationic surfactants as templates. The pores, which are periodically arranged in the material, are larger than in zeolites and can be functionalized, which offers new possibilities in applications such as catalysis, filtration, chemical separation, encapsulation.² Powders with different structures have been synthesized by adjusting the synthesis conditions^{3,4} and varying the surfactant nature.⁵

The synthesis of films (supported or not) with the same characteristics has been developed in order to make selective membranes and functionalized surface coatings. Such films can be prepared either in static conditions at solid/liquid or liquid/vapor interfaces^{6,7} or in dynamic conditions by spin- or dip-coating.^{8,9} In most cases, films were synthesized using the classic cetyltrimethylammonium bromide (CTAB) or chloride (CTAC) surfactant. Their structure was generally reported to be the 2D hexagonal MCM-41 type one with the pore channels aligned parallel to the substrate.

Only a few papers have reported the formation of films with a 3D pore network. Cubic phases were prepared using a large-headgroup cationic surfactant (cetyltriethylammonium bromide),¹⁰ triblock copolymers, or nonionic poly(ethylene oxide) surfactants.¹¹ 3D hexagonal structures were obtained using either a gemini surfactant^{10,12} or poly(ethylene oxide) surfactants.¹¹ Other 3D organizations were observed by calcination of CTAB templated films showing a lamellar type phase.⁸

We recently determined the experimental conditions to reproducibly prepare highly organized and textured CTAB

templated films by spin-coating on glass.¹³ We present here the complete structural characterization of these films by high resolution electron microscopy (HRTEM). This investigation unambiguously shows the formation of a 3D hexagonal phase, which could not have been discriminated from the well-known 2D hexagonal MCM-41 structure by the usual X-ray diffraction technique in the Bragg–Brentano geometry. This suggests that the formation of films in dynamic conditions leads to the stabilization of a new phase that does not belong to the phase diagram of CTAB in water.

Films were synthesized using the procedure previously described.¹³ The polymeric silica sol was prepared under acidic conditions by mixing TEOS ($\text{Si}(\text{OC}_2\text{H}_5)_4$), water ($\text{pH} = 1.25$) and ethanol in the 1:5:3.8 molar ratio, and aged 1 h at 60 °C. The CTAB was then dissolved into the sol with the CTAB/TEOS molar ratio equal to 0.1. The obtained solution was diluted with ethanol ($1/2$) and deposited on glass plates by spin-coating at 2000 rpm. In these conditions, highly ordered films of about 300 nm in thickness were obtained. The films were possibly calcined in air at 400 °C for 12 h, leading to the complete removal of organic species.

Films were characterized by X-ray diffraction (XRD) in the Bragg–Brentano geometry. Only one intense and sharp diffraction peak and its first harmonic appeared in the diffraction diagram, suggesting textured films. The same peak is observed for calcined films but shifted to larger 2θ values, indicating a contraction of 13% of the pore network perpendicular to the films.

HRTEM investigations were made using a Philips CM20 electron microscope operating at 200 kV with a point to point resolution $r = 0.27$ nm. The HRTEM images were slightly underfocused in order to enhance the contrast of the pores within the films. The order within the silica mesoporous films as well as their structure was studied by examining the films in plane view and in cross section.

[†] Ecole Polytechnique.

[‡] Laboratoire CNRS/Saint-Gobain "Surface du Verre et Interfaces".

[§] Universités Paris VI et Paris VII.

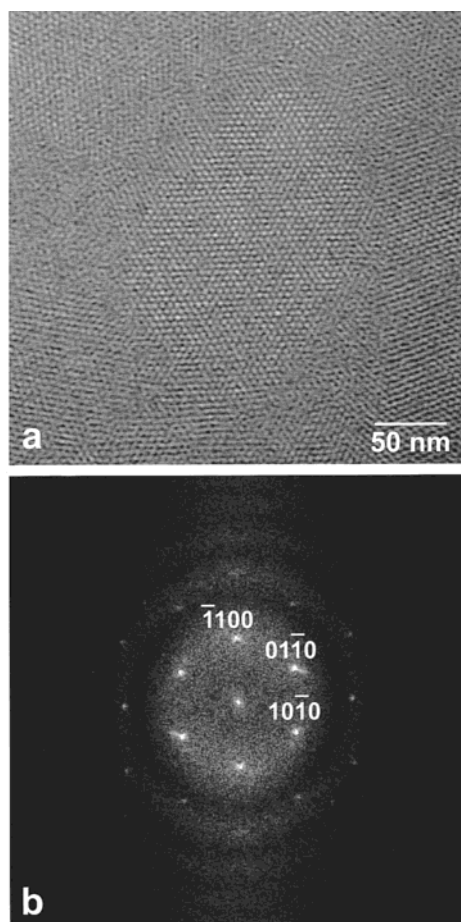


Figure 1. (a) HRTEM image of the uncalcined film in plane view. (b) Power spectrum ($=|\text{Fourier transform}|^2$) of the image showing the 6-fold symmetry. The indexes of the reflections belong to the $P6_3/mmc$ hexagonal phase. The zone axis is $[0001]$.

The structure of the films was determined from the computation of the power spectrum (i.e., square modulus of the Fourier transform) of the digitized HRTEM images of single domains in zone axis orientation (i.e., with one symmetry element parallel to the electron beam). Using such a procedure, the structural lattice parameters were obtained by measuring the interplanar angles and spacings from the corresponding diffraction vectors.

A typical in plane HRTEM view of an uncalcined film is shown in Figure 1a. The numerical diffractogram of this domain exhibits a 6-fold symmetry (Figure 1b). The length of each equivalent vector corresponds to a lattice spacing of 4.9 nm and angles between two equivalent reflections are 60° . The film is strongly textured, as shown in Figure 1a. HRTEM images of the cross-section film are shown in Figure 2a,b, and the corresponding power spectrum is presented in Figure 2c. From Figure 2a, it can be concluded that the organization process takes place over the whole film thickness and the stacking is perfect from the glass/film to the film/air interfaces. This leads to very sharp diffraction peaks in the power spectrum, as shown in Figure 2c. In this cross-section geometry, a lattice spacing of 3.5 nm is measured along the direction perpendicular to the plane of the film/glass interface. This value is in agreement with the one obtained from the corresponding X-ray diffraction pattern (3.7 nm). The in plane diffraction vector gives rise to a lattice distance of 5.0 nm. Finally, at 53° from the first vector, there is an additional diffraction peak that corresponds to a lattice distance of 4.1 nm (Figure 2c).

According to previous studies,^{8,9} the expected structure of our films is a 2D hexagonal stacking of cylindrical micelles

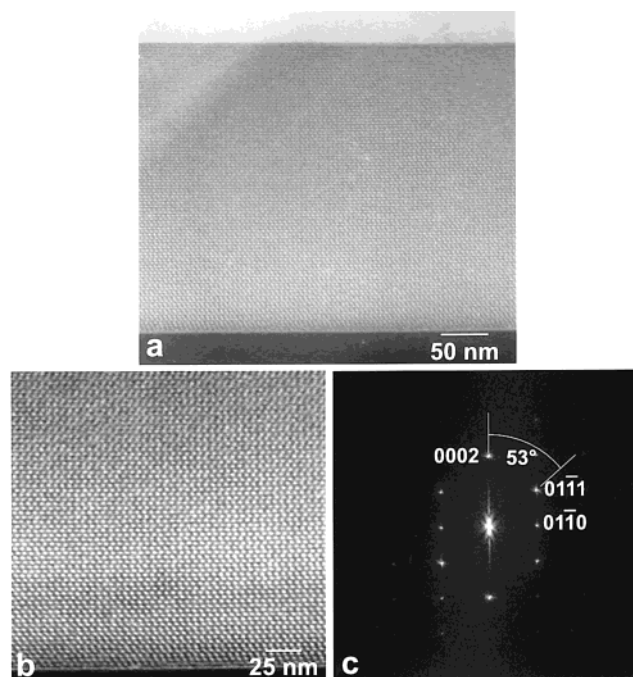


Figure 2. (a) HRTEM image of the uncalcined film in cross section. (b) Enlargement of the cross section showing the perfect ...ABAB... stacking sequence of the hexagonal phase parallel to the film/substrate interface. (c) Power spectrum of the image with the 2-fold symmetry. The indexes of the reflections belong to the hexagonal phase. The zone axis is $[1120]$.

with their axis oriented parallel to the film plane. This architecture is not compatible with the HRTEM observations presented here since two different diffraction patterns are observed in perpendicular directions with a common lattice distance. Moreover, as the film is strongly textured, this highly suggests that the presented numerical diffraction patterns (Figures 1b and 2c) correspond to the same structure observed in two perpendicular directions.

Two kinds of three-dimensional architectures are known for self-assembled surfactants: the hexagonal and the cubic phases. In our case, the 6-fold symmetry of the in plane numerical diffraction pattern (Figures 1b) is compatible with both the $[111]$ zone axis of the cubic structure and the $[0001]$ zone axis of the hexagonal one. However, among the perpendicular zone axes, the $[11\bar{2}0]$ hexagonal axis is the only one that fits the cross section diffractogram (Figure 2c). This excludes the cubic symmetry.

Assuming the 3D hexagonal structure, the projection along the $[0001]$ zone axis exhibits six equivalent $10\bar{1}0$ reflections at 60° . The a parameter of the hexagonal phase is given by $a = 2d_{10\bar{1}0}/\sqrt{3} = 5.6$ nm. The numerical diffraction pattern of the cross section (Figure 2c) corresponds to the $[1120]$ zone axis of the hexagonal phase. In such a projection, the c -axis of the hexagonal phase is perpendicular to the film plane. The $[11\bar{2}0]$ zone axis diffraction pattern displays the effect of the 6_3 screw axis in dynamical conditions of diffraction. The 0001 -type odd reflections along the c^* -axis, forbidden by 6_3 symmetry are effectively extinct when the zone axis is strictly parallel to the electron beam, which is the case here. The lattice pattern then displays the $c/2$ periodicity. The c parameter of the hexagonal structure for the uncalcined film is then equal to 7.0 nm.

These results allow us to determine the space group of the structure. The extinction of the 0001 reflection indicates the presence of a 6_3 axis parallel to the c direction of the hexagonal structure and there is a mirror plane perpendicular to this axis.

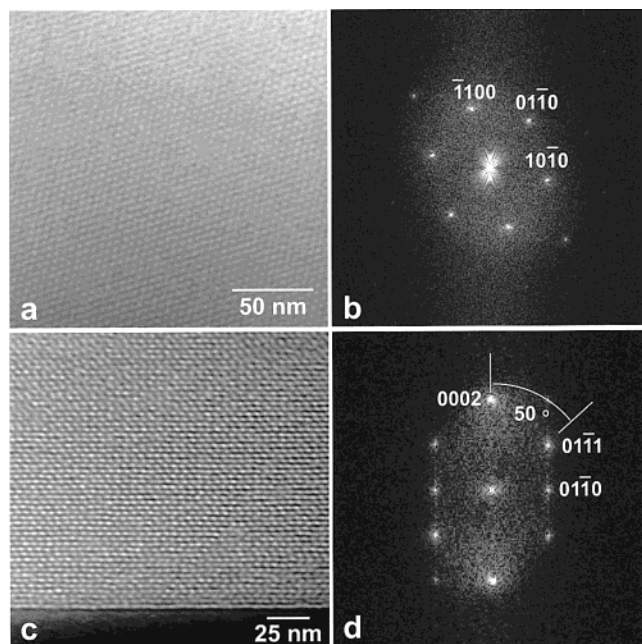


Figure 3. Calcined film. (a) Plane view HRTEM image. (b) Corresponding power spectrum with the 6-fold symmetry. The zone axis is [0001]. (c) Enlargement of the calcined film near the film/substrate interface observed in cross section. As in the uncalcined film, the stacking sequence parallel to the film/substrate interface is perfect. (d) Corresponding power spectrum with the 2-fold symmetry. The zone axis is [1120].

The plane view observations exhibit one family of mirror planes with their normal parallel to a (or b or $a + b$). The 6_3 axis and this family of mirror planes are the two generators of the space group. Consequently, the second family of mirror planes (with their normal parallel to $2a + b$) is necessarily a glide mirror of c type (i.e., with a $c/2$ translation parallel to the plane). Finally, the space group of the hexagonal structure studied here is $P6_3/mmc$ with $a = 5.6$ nm and $c = 7.0$ nm.

HRTEM images in plane view and in cross section of the calcined mesoporous film are shown in Figure 3a,c, respectively. The corresponding power spectra are presented in Figure 3b,d. Same symmetries have been obtained in the images and in the diffraction patterns before and after the thermal treatment. Thus, the ordered structure is maintained even after the removal of the surfactant molecules. According to the diffraction patterns, the structure lattice spacings of the calcined film are $a = 5.6$ nm and $c = 6.1$ nm.

This space group is the one observed in metals where the structure is described from the compact hard sphere model. In the present work, the c/a ratio of uncalcined films is equal to 1.25 (1.07 in the calcined film) and differs significantly from the well-known value of $2/3 \sqrt{6} = 1.63$ obtained in the close-packed hexagonal structure. This is consistent with the value of 53° (50° in the calcined film) measured for the angle between the 0002 and the 0111 reflections instead of 61.4° expected for the perfect structure.

We have synthesized CTAB templated silica films with a 3D hexagonal symmetry. This 3D organization is maintained after the removal of the surfactant molecules by calcination leading to original mesoporous materials. The obtention of such

a film structure is not easy to understand, as the corresponding phase does not exist in the phase diagram of CTAB in water nor in other solvents.¹⁴ This contrasts with mesoporous silica powders made with CTAB or CTAC, which exhibit 2D hexagonal, cubic, or lamellar structures like in the surfactant phase diagrams,^{1,3} and also with CTAB films synthesized under static conditions, which always present a 2D hexagonal structure.^{6,15–17} In fact, 3D hexagonal structures have only been reported using other templates such as gemini surfactants.^{5,18}

In our case, the stabilization of a highly oriented 3D hexagonal structure obtained with CTAB should be specific of the dynamic conditions used for the elaboration of films. The solvent evaporation due to the spin-coating process implies the freezing of the micellar organization existing in the sol at the silica gelation. The observed 3D structure could then be explained by the hexagonal packing of spherical micelles just as in colloidal crystals. But, in these systems, the interspace between spherical micelles is filled by polymeric silica walls. Compared to the close-packed structure, this leads to weaker values of the c/a hexagonal ratio due to the constrained one-dimensional shrinkage of the films normal to the substrate plane.¹³ Finally, note that the original structure presently described in spin-coated films should result from the favorable experimental conditions used for their elaboration, allowing us to concentrate spherical micelles while preventing their natural evolution toward tubules.

Acknowledgment. This work was partially supported by Saint-Gobain Recherche.

References and Notes

- (1) Beck, J. S.; Vartuli, J. C.; Roth, W. J.; Leonowicz, M. E.; Kresge, C. T.; Schmitt, K. D.; Chu, C. T.-W.; Olson, K. H.; Sheppard, E. W.; McCullen, S. B.; Higgins, J. B.; Schlenk, J. L. *J. Am. Chem. Soc.* **1992**, *114*, 10834.
- (2) Beck, J. S.; Vartuli, J. C. *Curr. Opin. Solid State Mater. Sci.* **1996**, *1*, 76.
- (3) Monnier, A.; Schüth, F.; Huo, Q.; Kumar, D.; Margolese, D.; Maxwell, R. S.; Stucky, G. D.; Krishnamurty, M.; Petroff, P.; Firouzi, A.; Janicke, M.; Chmelka, B. F. *Science* **1993**, *261*, 1299.
- (4) Vartuli, J. C.; Schmitt, K. D.; Kresge, C. T.; Roth, W. J.; Leonowicz, M. E.; McCullen, S. B.; Hellring, S. D.; Beck, J. S.; Schlenk, J. L.; Olson, K. H.; Sheppard, E. W. *Chem. Mater.* **1994**, *6*, 2317.
- (5) Huo, Q.; Margolese, D. I.; Stucky, G. D. *Chem. Mater.* **1996**, *8*, 1147.
- (6) Yang, H.; Coombs, N.; Sokolov, I.; Ozin, G. *Nature* **1996**, *381*, 589.
- (7) Aksay, I. A.; Trau, M.; Manne, S.; Honma, I.; Yao, N.; Zhou, L.; Fenter, P.; Eisenberg, P. M.; Gruner, S. M. *Science* **1996**, *273*, 892.
- (8) Lu, Y.; Gangull, R.; Drewlen, C. A.; Anderson, M. T.; Brinker, C. J.; Gong, W.; Guo, Y.; Soye, H.; Dunn, B.; Huang, M. H.; Zink, J. I. *Nature* **1997**, *389*, 364.
- (9) Ogawa, M.; Ishikawa, H.; Kikuchi, T. *J. Mater. Chem.* **1998**, *8*, 1783.
- (10) Zhao, D.; Yang, P.; Margolese, D. I.; Chmelka, B. F.; Stucky, G. D. *Chem. Commun.* **1998**, 2499.
- (11) Zhao, D.; Yang, P.; Melosh, N.; Feng, J.; Chmelka, B. F.; Stucky, G. D. *Adv. Mater.* **1998**, *10*, 16, 1380.
- (12) Tolbert, S. H.; Schäfer, T. E.; Feng, J.; Hansma, P. K.; Stucky, G. D. *Chem. Mater.* **1997**, *9*, 1962.
- (13) Besson, S.; Gacoin, T.; Jacquiod, C.; Ricolleau, C.; Babonneau, D.; Boilot, J.-P. *J. Mater. Chem.* **2000**, *10*, 1331.
- (14) Auvray, X.; Petipas, C.; Anthore, R. *J. Phys. Chem.* **1989**, *93*, 7458.
- (15) Miyata, H.; Kuroda, K. *Adv. Mater.* **1999**, *11*, No. 10, 857.
- (16) Holt, S. A.; Foran, G. J.; White, J. W. *Langmuir* **1999**, *15*, 2540.
- (17) Miyata, H.; Kuroda, K. *Chem. Mater.* **2000**, *12*, 49.
- (18) Huo, Q.; Leon, R.; Petroff, P. M.; Stucky, G. D. *Science* **1995**, *268*, 1324.